Available online at www.sciencedirect.com
ScienceDirect
Journal of Sound and Vibration 300 (2007) 916–931
JOURNAL OF SOUND AND VIBRATION
www.elsevier.com/locate/jsvi

Friction-induced oscillations of a slider: Parametric study of some system parameters

M. Nadim Ahmed Emira*

Mechanical Design & Production Department, Faculty of Engineering, Zagazig University, 44519 Zagazig, Egypt

Received 10 September 2004; received in revised form 11 September 2006; accepted 12 September 2006
Available online 30 October 2006

Abstract

A typical frictionally excited pin on disk system is modeled as a basis for vibration control. The model is based on chosen experimental setup parameters. The analysis incorporates normal, tangential and torsional degrees of freedom. The effect of varying both the normal force and the pin stiffness on the response of the pin subsystem in all directions is investigated numerically. A detailed parametric study shows that the operating condition namely the normal force and the rotational speed have a remarkable influence on the response. A correlation between measured and calculated system response is presented, that supports the validity of the presented model. The dynamic characteristics of the system, namely stiffness of the pin in both normal and torsional direction, have no significant effect on its response, while its tangential stiffness has a minor effect.

1. Introduction

Friction-induced vibration, chatter, and squeal are serious problems in many industrial applications. Many experimental and analytical studies have led to insight on the factors contributing to the brake squeal or to the improvement of squeal in disk brakes of a specific type or in a particular make and model of automobile. Experimental studies have accumulated a wealth of information about the nature of squeal, the vibration modes therein, the wear of brake components, and frictional interactions in brakes. Analytical studies have provided useful insights into how friction laws, geometry and the dynamics of brake components can lead to squeal or instability in simple models of disk brakes. Finite elements have been used to try to extend these insights to more accurate brake models. There is a large body of models devoted to brake squeal.

An early detailed analysis of a model for a squealing disk brake was presented by Jarvis and Mills [1]. Then, models for squealing disk brakes have featured an increased number of degrees of freedom, increased complexity, and often, more complex friction models. Many studies about friction mechanisms have been reported.

Early work of Earles and Lee [2] featured experiments where a disk, contacted by a pin which is supported by a flexible cantilever, is spun at a constant speed. They stated that the system stability is dependent on the

*Tel.: +20 55 2345995; fax: +20 55 2304987.
E-mail address: nadimemira@hotmail.com.

0022-460X/$ - see front matter © 2006 Elsevier Ltd. All rights reserved.
doi:10.1016/j.jsv.2006.09.010

coefficient of friction. Earles and Badi [3] and Earles and Chambers [4,5] used pin on disk systems in which two pins were acting on the disk to investigate and quantify the sprag-slip mechanism for squeal. The investigations performed consisted of examining how the damping influenced squeal. In these works, a linear stability analysis was performed on lumped parameter models of pin-disk systems in order to find the flutter boundaries in parameter space. After the constraints had been incorporated, these models were generally linear three- or five-degree-of-freedom systems. They found that damping in the pin assembly (corresponding to damping of the brake pad assembly in a disk brake) could enlarge the unstable regions under certain circumstances, while disk damping always reduced these regions.

From the perspective of computational mechanics, Oden and Martins [6] presented comprehensive reviews of friction models. They showed that the computation of the true contact can be modeled through direct numerical simulations.

The experimental tests on a pin-on disk type sliding system by Dweib and D'Souza [7] have indicated that, for a constant sliding speed, the friction force depends on the normal load. They showed that according to the value of the normal load, there are four different regimes, namely: steady-state, nonlinear, transient friction regions and self-excited vibration region. Dweib and D'Souza [8] presented, based on experimental results an empirical model of contact mechanics. This empirical model has been developed for the region of self-excited vibrations. Their results concluded that, the mechanism that causes self-excited vibrations in their model is the coupling between its degrees of freedom.

Ibrahim [9], addressed friction and contact mechanics. He summarized the principal results pertaining to factors affecting friction between sliding surfaces. According to him, the occurrence of stick-slip is unpredictable and is attributed to the fact that the slope of the friction-speed curve is not constant but varies randomly with contamination, surface finish, miss-alignment of sliding surfaces, and other factors. He classified vibrations in the mechanical systems into three categories: stick-slip, vibrations induced by random surface irregularities and quasi-harmonic self-excited oscillations. Ibrahim et al. [10] measured the average normal and friction forces acting on a friction element (in the form of a dowel) which was placed in contact with a rotating disk. Both the rotation speed and direction of the disk were variable, and their tests were performed at constant rotational speeds. They noted several interesting features. Most notably, neither the normal force nor the kinetic coefficient of friction were constant. In fact, these authors reported that the friction and normal forces acting on the friction element are random and non-Gaussian processes. They also developed a single-degree-of freedom model for the vibration of the friction element. This model was subsequently analyzed in further detail by Qiao and Ibrahim [11]. Ibrahim [12] has discussed the relationships between the results of Ibrahim et al. [10] and Qiao and Ibrahim [11] and role of random vibrations in the generation of brake noise.

Considering the acoustics of friction-induced vibration, an illuminating discussion has been reported by Akay [13]. He attempted to bring together acoustics and friction by exposing many of the topics that are common to both fields. He affirmed that modeling of friction-induced vibrations and friction damping in mechanical systems requires an accurate description of friction for which only approximations exist. An experimental investigation of friction-induced noise and vibration using a pin-on-disk set-up was presented by Emira and Uras [14]. Their results indicated that the average normal force has a significant effect on the system response that caused generating noise under self-excited vibration. They showed that introducing external excitation to their system has a positive influence on the system response measured in terms of system noise. Kinkaid et al. [15] presented a detailed revision of the pin-on-disk friction models. He demonstrated a revision of most of the models that have appeared in the literature, and summarized some of them. He also pointed out the inter-relationships between these models. In these models, a linear stability analysis was performed in order to predict the onset of instability which, according to most researchers, have been correlated to the occurrence of squeal.

Considering the dynamic instabilities of the pin-on-disk system, Mote [16] studied the case of a stationary flexible disk subjected to a rotating load. On the other hand, Iwan and Moeller [17] studied the dynamic instability of a rotating flexible disk subjected to a stationary load. For both cases, either of which is rotating, the system may become unstable at certain values of the mass–spring–damper system. Further investigation of factors affecting resonance of stationary disk excited by a rotating load, were carried out by Shen [18]. Tworzydlo et al. [19] presented a numerical study of dynamic instabilities of mechanical systems

with friction-induced vibrations, self-excited oscillations and stick-slip motion. They modeled a typical pin-on-disk apparatus as the assembly of rigid bodies with elastic connections to represent the properties of the interface. In the analysis of stability of frictional sliding, they followed the general procedure used by Oden and Martins [6]. Shin et al. [20] adopted a two degrees-of-freedom model, where the disk and the pad are modeled as single modes connected by a sliding friction interface. They investigated the detailed dynamical behavior of the model for various combinations of both friction and system parameters.

Mottershead has published a series of articles on instabilities in annular disks to which a rotating system of a discrete mass-dashpot-spring and an accompanying frictional follower force was applied. A thorough review of this work is summarized in the review article by Mottershead [21] and its relationship to a floating caliper brake system is outlined by Ouyang and Mottershead [22]. Chan et al. [23] presented a theory of brake squeal which is based on the splitting of the frequency of the doublet modes in the symmetric disk when a friction force is applied, this splitting could lead to flutter which is associated to brake squeal. They considered a clamped elastic annular disk which is loaded (at a discrete number of points) by a tangential follower force traction which is related to the normal pressure by the coefficient of friction. Using a finite element model for the disk, they developed a model for the linear vibrations of the stationary disk subject to the tangential follower forces. Chan et al. [24] investigated the instabilities in annular disks to which a rotating system of a discrete mass-dashpot-spring and an accompanying frictional follower force was applied. Their model is related, by a coordinate change, to the dual model of a rotating plate acted upon by a fixed load system, provided the simple plate model to be used. In other words, the deformation induced in the plate by the rigid rotation is not considered in the dual model.

Mottershead and Chan [25] showed that follower friction force led to flutter instability indicated by the combining of eigenvalues using a distributed frictional load. Mottershead [21] analyzed the instabilities due to frictional follower forces and friction-induced parametric resonance. An extension of this study to the case with negative friction-velocity slope is also carried out by Ouyang et al. [26]. They investigated parametric resonance under a sector load rotating on an annular disk (with friction) and they identified combination resonance and how it changes when friction has a negative slope with respect to velocity. They also addressed the tendency of a disk to generate noise when the natural frequencies of in-plane and bending vibrations exist close to each other. as well as self-excited vibrations of a circular plate with friction forces acting on its edge to model squeal in drum brakes [27]. These papers focus on the parametric resonance induced in the disk by the rotating system.

Ouyang et al. [28–30] presented a notable work in the vein of assuming constant friction coefficient and self-excited vibrations. They developed a finite element model for the brake pad assemblies, calipers and piston of a floating caliper disk brake and a plate model for the brake rotor. They considered the effects of the rotation of the disk rotor. In their finite element model, they considered the flexibilities of the rotor and the brake pad assemblies. As these bodies deform during the vibrations of the disk brake system, a variation in the normal forces between them occurs. This in turn causes a variation in the friction forces even if the coefficient of friction is constant.

A broad illustration of the effect of some of the geometric and operating parameters on the friction-induced vibration of the pin-on-disk system is the ultimate aim of this study, with a future thought of using passive control methodology to limit or reduce its vibration. A mathematical model in which the pin is considered as an elastic element with stiffness k_1, k_2 and k_3 while the disk is of higher rigidity is introduced. The predicted system response is correlated to experimental system response measured in terms of system noise [14].

In this present work the responses of the rotating pin in three directions are investigated in terms of speed of rotation, applied normal force and its stiffness.

2. Pin-on-disk system modeling

An analytical model of the rotating pin, of the pin-on-disk system shown in Fig. 1, is presented. The pin axis is normal to the disk surface. The pin represented by a mass m and a moment of inertia I about a central axis through its mass center O, has the displacements X, Y and ϕ. The rotation ϕ is associated with pin's torsional stiffness k_3. The tip of the pin is distanced L vertically from O (mass center of the pin). The spherical pin tip and the rigid stationary disk surfaces are hardened to 58-62 HRC with surface roughness average (Ra) of

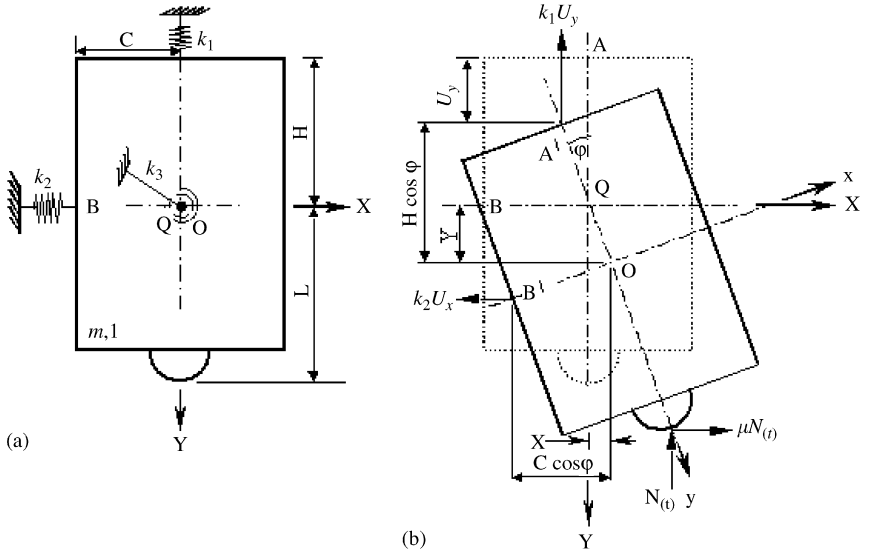

Fig. 1. Pin-on-disk system modeling.

0.025. As shown in Fig. 1(a), a set of fixed axes $QXYZ$ are coincident with the set of moving coordinate axes $Oxyz$, which are attached to the pin subsystem. The direction of both the friction and the normal forces on the pin's tip are the x- and the y-axis, respectively. The three degrees of freedom correspond to the translations in both the normal and frictional directions and torsional rotation about the z-axis.

It is assumed that the relative sliding between the pin and the disk is unidirectional and finite at all time. Hence, the friction force always acts in the same direction. The reacted normal force on the pin's tip acts vertically upwards. It is assumed that these directions are fixed at all times. It is also assumed that the contact between the pin and the disk is maintained at all times. The stiffness k_1 and k_2 are attached from the points A and B, respectively. Fig. 1(b) shows the pin subsystem deflected from its static position. From the geometric compatibility of the pin subsystem, the displacements U_y and U_x of points A and B, are given by

$$U_x = X + C(1 - \cos\phi),$$
$$U_y = Y + H(1 - \cos\phi). \tag{1}$$

The equations of motion in the X, Y and ϕ directions are written as follows:

$$m\ddot{X} + k_2U_x - \mu N_{(t)} = 0,$$
$$m\ddot{Y} + k_1U_y + N_{(t)} = 0,$$
$$I\ddot{\phi} + (k_3 + k_2XC + k_1YH - N_{(t)}L)\phi - \mu N_{(t)}L = 0. \tag{2}$$

Substituting Eq. (1) into Eq. (2) and for very small ϕ, such that $\sin\phi \simeq \phi$ and $\cos\phi \simeq 1$, then Eq. (2) becomes

$$m\ddot{X} + k_2X - \mu N_{(t)} = 0,$$
$$m\ddot{Y} + k_1Y - N_{(t)} = 0,$$
$$I\ddot{\phi} + (k_3 + k_2XC + k_1YH - N_{(t)}L)\phi - \mu N_{(t)}L = 0. \tag{3}$$

According to Qiao and Ibrahim [11] and the reported results of Emira and Uras [14], the dependence of the friction coefficient on the relative sliding velocity, shown in Fig. 2, may be represented by the cubic polynomial:

$$\mu = a_0\,\mathrm{sgn}\,(V - w) + a_1(V - w) + a_3(V - w)^3, \tag{4}$$

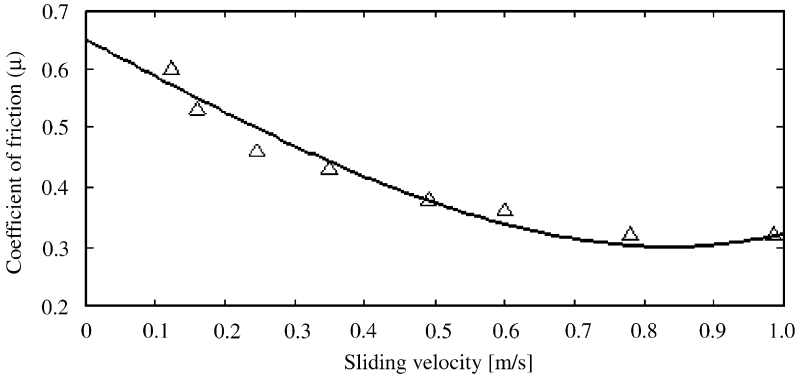

Fig. 2. Coefficient of friction versus sliding velocity (data from Ref. [14]): (———) curve fitting and (△———△) experimental.

where V is the pin rotational velocity at the contact point, and w is the velocity of the frictional element (the velocity response of the pin due to its flexibility), at the same point of contact. From the model geometry shown in Fig. 1, the displacement of the pin tip is $(X + L \sin \phi)$, then the velocity is given by $w = \dot{X} + L\dot{\phi}$.

The coefficients a_0, a_1 and a_3 are mainly governed by the conditions of the sliding surfaces and their material properties. By applying the least-square curve fitting to the experimental data obtained by Emira and Uras [14], one can get the cubic polynomial coefficients as follows: $a_0 = 0.649$, $a_1 = -0.623$ and $a_3 = 0.297$.

In order to transform each of the second-order DE, namely Eq. (3), into two simultaneous first-order DE, the following expressions are introduced:

$$u = \dot{X}, \quad v = \dot{Y} \quad \text{and} \quad \theta = \dot{\phi}. \tag{5}$$

Consequently $w = u + L\theta$, $\dot{u} = \ddot{X}$, $\dot{v} = \ddot{Y}$ and $\dot{\theta} = \ddot{\phi}$. Substituting these values in Eq. (3), and rearranging gives

$$\begin{aligned}
\dot{u} &= \frac{\mu N_{(t)}}{m} - \frac{k_2}{m} X, \\
\dot{v} &= -\frac{k_1}{m} Y - \frac{N_{(t)}}{m}, \\
\dot{\theta} &= \frac{\mu N_{(t)} L}{I} - \frac{\phi}{I}(k_3 + k_2 XC + k_1 YH + N_{(t)} L).
\end{aligned} \tag{6}$$

The setup dynamic characteristics parameters used, abstracted from experimental investigation by Emira and Uras [14], are as follows: the normal stiffness $k_1 = 15.44 \times 10^3\,\mathrm{N\,m^{-1}}$, the tangential stiffness $k_2 = 2.465 \times 10^5\,\mathrm{N\,m^{-1}}$ and the torsional stiffness $k_3 = 67.275\,\mathrm{N\,m\,rad^{-1}}$. The mass of the pin $m = 0.625\,\mathrm{kg}$ and the range of the average normal force $N_{(t)} = (25-55)\,\mathrm{N}$. The geometric dimensions of the pin are: $C = 0.01\,\mathrm{m}$, $L = 0.09\,\mathrm{m}$ and $H = 0.0836\,\mathrm{m}$. The mass moment of inertia of the pin $I = 6.69 \times 10^{-4}\,\mathrm{kg\,m^2}$. The rotating velocities of the pin considered are 50, 100 and 150 rev/min.

3. Solution of equations of motion

The numerical solution of the sliding system can be obtained by applying the central difference method with the initial conditions $u_0, X_0, v_0, Y_0, \theta_0, \phi_0$ as mentioned in Ref. [31]. Denoting the response as: $X_i = X(t = t_i)$, $X_{i+1} = X(t = t_{i+1})$ and $X_{i-1} = X(t = t_{i-1})$, respectively. These notations apply for response in all directions.

To start the numerical calculation (at time $t = t_1 = \Delta t$) the first value of each of the state variables is calculated using a first-order Taylor expansion as $X_1 = X_0 + \Delta t\, \dot{X}_0$, $Y_1 = Y_0 + \Delta t\, \dot{Y}_0$ and $\phi_1 = \phi_0 + \Delta t\, \dot{\phi}_0$, etc. Then, the values of the state variables at time $t = t_2 = t_1 + \Delta t$ and higher are calculated using the central difference method, where Eq. (5) can be rewritten as: $u_i = X_{i+1} - X_{i-1}/2\Delta t$, $v_i = Y_{i+1} - Y_{i-1}/2\Delta t$ and $\theta_i = \phi_{i+1} - \phi_{i-1}/2\Delta t$, which can be rearranged as follows:

$$X_{i+1} = 2\Delta t u_i + X_{i-1}, \quad Y_{i+1} = 2\Delta t v_i + Y_{i-1} \text{ and } \phi_{i+1} = 2\Delta t \theta_i + \phi_{i-1} \tag{7}$$

and Eq. (6) is rewritten as follows:

$$\frac{u_{i+1}-u_{i-1}}{2\Delta t}=\frac{\mu N_{(t)}}{m}-\frac{k_2}{m}X_i,$$
$$\frac{v_{i+1}-v_{i-1}}{2\Delta t}=-\frac{k_1}{m}Y_i-\frac{N_{(t)}}{m},$$
$$\frac{\theta_{i+1}-\theta_{i-1}}{2\Delta t}=\frac{\mu N_{(t)}L}{I}-\frac{\phi_i}{I}(k_3+k_2X_iC+k_1Y_iH-N_{(t)}L), \tag{8}$$

where $\mu=a_0\,\mathrm{sgn}\,(V-u_i-L\theta_i)+a_1(V-u_i-L\theta_i)+a_3(V-u_i-L\theta_i)^3$.

Eq. (8) is rearranged in the following form:

$$u_{i+1}=\frac{2\Delta t\,\mu N_{(t)}}{m}-\frac{2\Delta t\,k_2}{m}X_i+u_{i-1},$$
$$v_{i+1}=\frac{-2\Delta t\,k_1}{m}Y_i-\frac{2\Delta tN_{(t)}}{m}+v_{i-1},$$
$$\theta_{i+1}=\frac{2\Delta t\,\mu N_{(t)}L}{I}-\frac{2\Delta t}{I}(k_3+k_2X_iC+k_1Y_iH-N_{(t)}L)\phi_i+\theta_{i-1}. \tag{9}$$

Then the equations which represent the state variables of the system, namely Eqs. (7) and (9) are rearranged in the following matrix forms:

$$\mathbf{R}_{i+1}=\mathbf{A}\mathbf{R}_i+\mathbf{B}\mathbf{R}_{i-1}+\mathbf{P}, \tag{10}$$

where

$$\mathbf{R}_{i+1}=\begin{bmatrix}X_{i+1}\\Y_{i+1}\\\phi_{i+1}\\u_{i+1}\\v_{i+1}\\\theta_{i+1}\end{bmatrix},\quad \mathbf{R}_i=\begin{bmatrix}X_i\\Y_i\\\phi_i\\u_i\\v_i\\\theta_i\end{bmatrix},\quad \mathbf{R}_{i-1}=\begin{bmatrix}X_{i-1}\\Y_{i-1}\\\phi_{i-1}\\u_{i-1}\\v_{i-1}\\\theta_{i-1}\end{bmatrix},\quad \mathbf{A}=\begin{bmatrix}0&0&0&A_{14}&0&0\\0&0&0&0&A_{25}&0\\0&0&0&0&0&A_{36}\\A_{41}&0&0&0&0&0\\0&A_{52}&0&0&0&0\\0&0&A_{63}&0&0&0\end{bmatrix},$$

$$\mathbf{B}=\begin{bmatrix}1&0&0&0&0&0\\0&1&0&0&0&0\\0&0&1&0&0&0\\0&0&0&1&0&0\\0&0&0&0&1&0\\0&0&0&0&0&1\end{bmatrix},\ \text{and}\ \mathbf{P}=\begin{bmatrix}0\\0\\0\\P_{14}\\P_{15}\\P_{16}\end{bmatrix}.$$

The values of the different elements are as follows:

$$A_{14}=A_{25}=A_{36}=2\Delta t,\quad A_{41}=-2\Delta tk_2/m,\quad A_{52}=-2\Delta tk_1/m,$$

$$A_{63}=-2\Delta t(k_3+k_2CX_i+k_1HY_i-N_{(t)}L)/I,$$

$$P_{14}=2\Delta t\,N_{(t)}\{a_0\,\mathrm{sgn}(V-u_i-L\theta_i)+a_1(V-u_i-L\theta_i)+a_3(V-u_i-L\theta_i)^3\}/m,$$

$$P_{15}=-2\Delta t\,N_{(t)}/m\ \text{and}$$

$$P_{16}=-2\Delta t\,N_{(t)}L\{a_0\,\mathrm{sgn}(V-u_i-L\theta_i)+a_1(V-u_i-L\theta_i)+a_3(V-u_i-L\theta_i)^3\}/I.$$

4. Results and discussions

The study investigates the effect of varying both the normal force and the stiffness of the pin, on the steady-state response. In this context the "steady-state response" stands for the response at the end time domain used. Primary investigations showed that the oscillatory response of the pin in all directions completely disappears after about 3.5 s. For that reason a time domain of 6 s, was used to ensure that the system has almost reached a steady-state shape. All the results were taken at the end of the chosen time interval for reason of comparison.

The studied range of variation of the dynamic characteristics; namely stiffness, is within $\pm 20\%$ of the experimental setup parameters. The values of the applied normal force vary between 25 and 55 N, at three different rotational speeds.

The equations of motion of the numerical model are solved using the central difference method, with chosen time domain $T = 6$ s. Achieving stability using the central difference scheme [31], implies using a time step Δt smaller than a critical value $\Delta t_{cr} = \tau/10$, where τ is the periodic time of the upper frequency of interest (2 kHz).

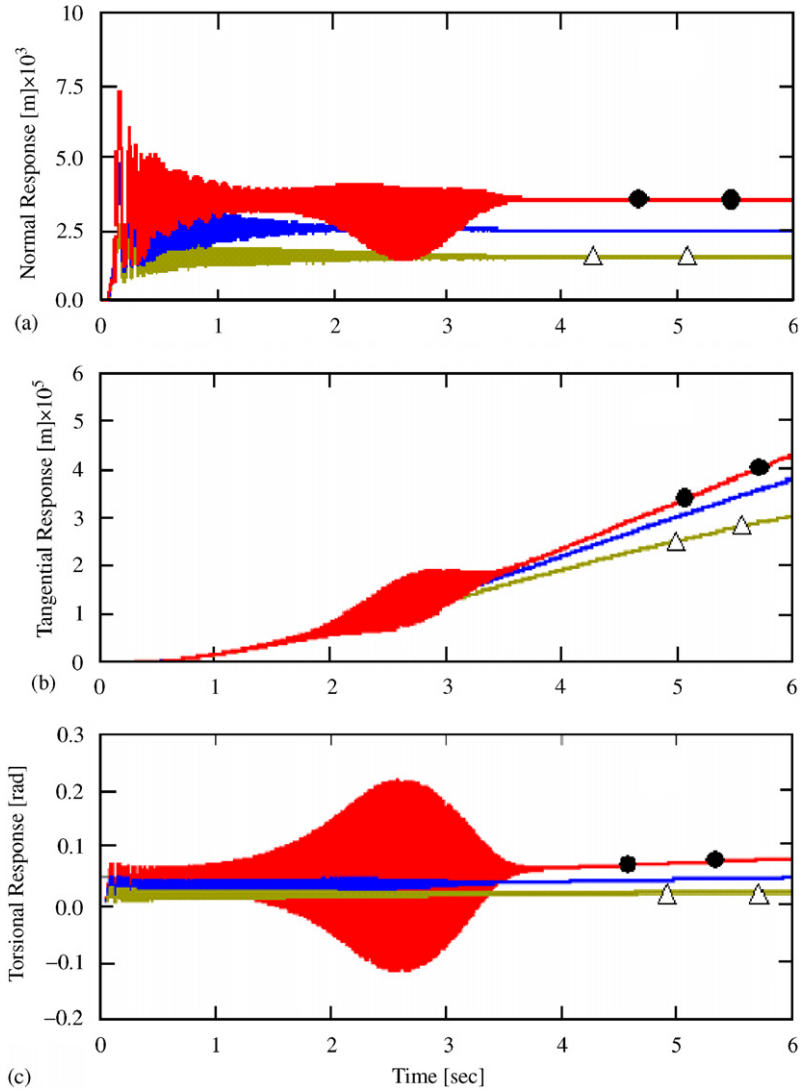

Fig. 3. Effect of varying the normal force on system response in the three directions: (a) vertical, (b) horizontal and (c) torsional, at 100 rev/min, (●——●) 55 N, (———) 40 N and (△——△) 25 N.

4.1. Effect of changing the normal force on the response

Fig. 3 displays the dynamic response, at three different values of the normal force 25, 40 and 55 N, in three directions: vertical, tangential and torsional at 100 rev/min. The figure shows that; in general, increasing the normal force increases the system steady-state response in all directions. It also shows that a dominant self-excited vibration occurs near the middle of the taken time period as a result of increasing the normal force up to 55 N.

Fig. 4 shows the relationship between the steady-state amplitude of response in the normal, tangential and torsional directions versus the normal force, at three different rotational speeds namely, 50, 100 and 150 rev/min. At 100 rev/min rotational speed, increasing the normal force by 20%, increases the normal amplitude by around 21%, the tangential amplitude by 8% and the torsional amplitude by 16%. These results indicate that the normal force has a great influence on the response of the system in the three directions. The figure shows that increasing the rotational speed, decreases the system response in the three directions.

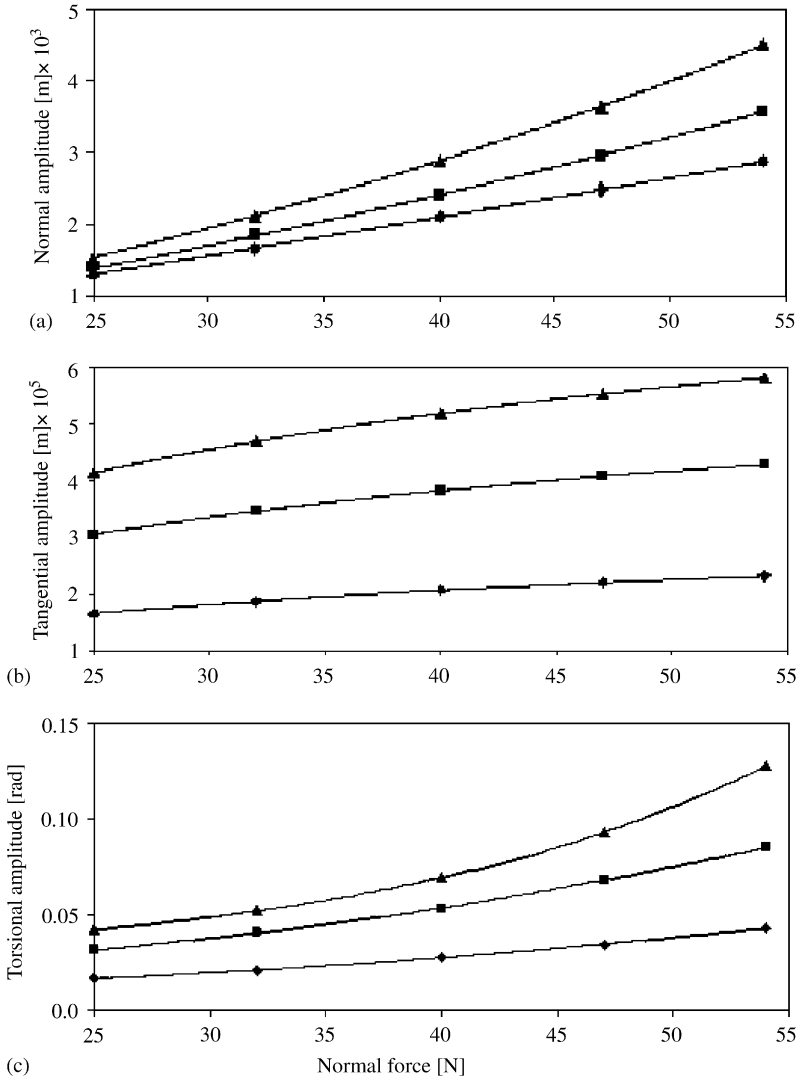

Fig. 4. System steady-state response; versus normal force, in the three directions at different rotational velocities: (a) vertical, (b) horizontal and (c) torsional, at three rotational velocities, (—▲—) 50 rev/min, (—■—) 100 rev/min and (—◆—) 150 rev/min.

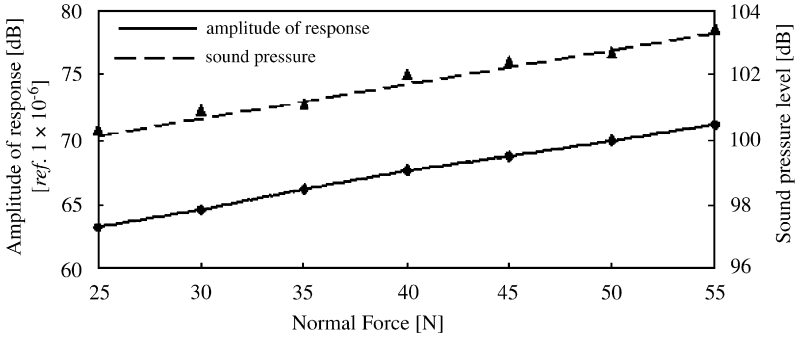

Fig. 5. Correlation between calculated system response (———) in the normal direction and measured sound pressure level (— —) [14], at 100 rev/min.

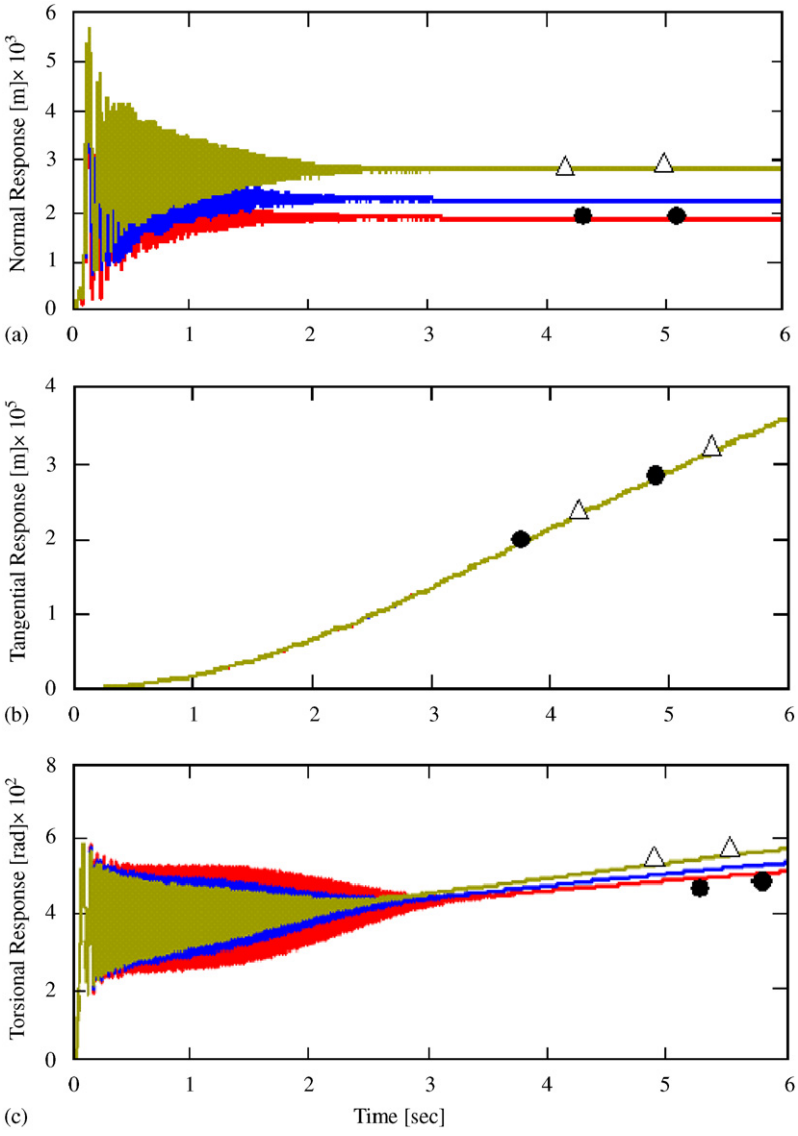

Fig. 6. Effect of varying normal stiffness k_1 on system response; at 35 N applied normal force and 100 rev/min, in the three directions: (a) vertical, (b) horizontal and (c) torsional: (△———△) −20%, (———) setup value of k_1 and (●———●) +20%.

As explained in Ref. [32], the sound pressure level is related to the vibration parameters of a specific vibrating surface. A correlation is established between the measured sound pressure level [14], and the corresponding numerically predicted system vibrational response in the normal direction. The system response in the normal direction and the near field measured sound pressure level is shown in Fig. 5. A high correlation between the two quantities is observed in the figure. This correlation gives a high indication of the correctness of the prediction of the presented model.

4.2. Effect of changing the normal stiffness on the response

Fig. 6 shows the effect of changing the normal stiffness k_1 on the time history of normal, tangential and torsional response amplitudes, at rotational speed of 100 rev/min and a chosen normal force valued 35 N. In Fig. 6(a), it can be noticed that, as the normal stiffness increases, the steady-state amplitude of response in the normal direction decreases. Fig. 6(b) shows the time history of the tangential response at different values of

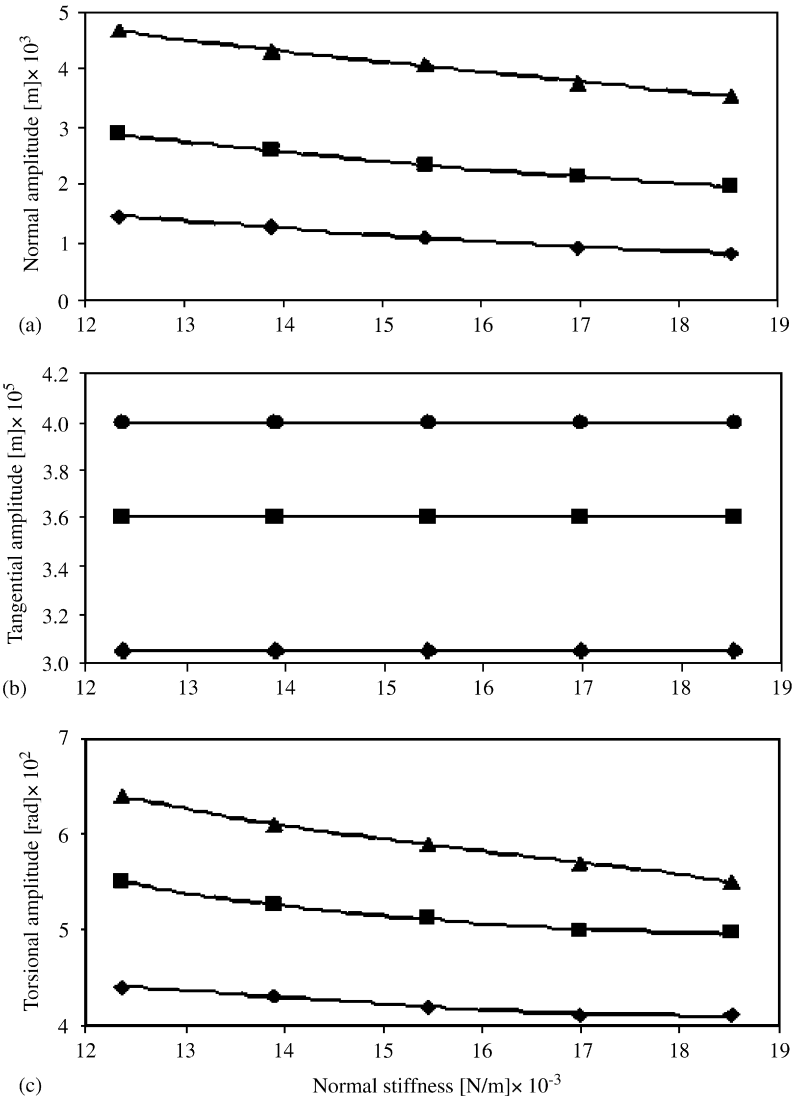

Fig. 7. System steady-state response versus normal stiffness at 100 rev/min; in the three directions: (a) vertical, (b) horizontal and (c) torsional, at three applied normal forces, (—▲—) 45 N, (—■—) 35 N and (—◆—) 25 N.

normal stiffness. In this case, changing the normal stiffness does not change the tangential response amplitude. Fig. 6(c) shows a decrease in the steady-state amplitude of response in the torsional direction as the normal stiffness increases.

Fig. 7 shows the response versus normal stiffness k_1 at three different values of the normal force at 100 rev/min. In Fig. 7(a), it is shown that as the normal stiffness increases by 10%, the steady-state amplitude of response in the normal direction decreases by around 9%. The tangential amplitude of response is not affected by the change in the normal stiffness, as shown in Fig. 7(b). The steady-state amplitude of response in the torsional direction decreases by around 2.5% due to an increase of 10% in the normal stiffness as shown in Fig. 7(c). Generally, these results show that changing the normal stiffness affects the response in both normal and torsional directions only, with a reflective effect on the normal response.

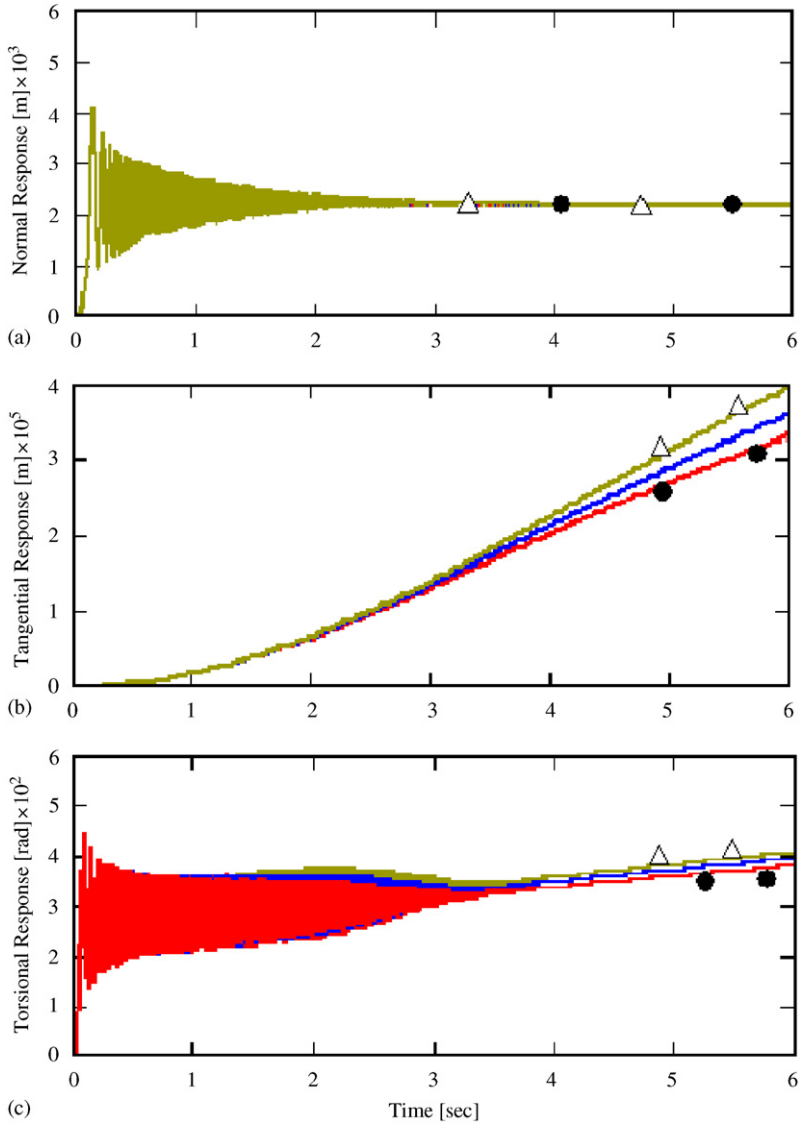

Fig. 8. Effect of varying tangential stiffness k_2 on system response; at 100 rev/min and 35 N applied normal force, in the three directions: (a) vertical, (b) horizontal and (c) torsional, (△——△) −20%, (——) setup value of k_2 and (●——●) +20%.

4.3. Effect of changing the tangential stiffness on the response

The effect of changing the tangential stiffness k_2 in a range of $\pm 20\%$ of the setup value, is investigated. Fig. 8 shows the time history of normal, tangential and torsional amplitudes of response, due to changing of the tangential stiffness k_2, at rotational speed of 100 rev/min and normal force of 35 N. It can be seen from Fig. 8(a) that changing the tangential stiffness has no effect on the normal response. An inverse relation between the change in the tangential stiffness and the steady-state amplitude of response in both the tangential and torsional directions is shown in Figs. 8(b) and (c).

Fig. 9 shows the response versus tangential stiffness k_2 at three different values of the normal force at 100 rev/min. In Fig. 9(a), it is found that the amplitude of response in the normal direction remains without any change. Fig. 9(b) shows that the steady-state amplitude of response in the tangential direction decreases by around 5.5% for a 10% increase of the tangential stiffness. A similar change in the tangential stiffness, leads to a decrease of the steady-state amplitude of response in the torsional direction by around 3.5%, as shown in Fig. 9(c).

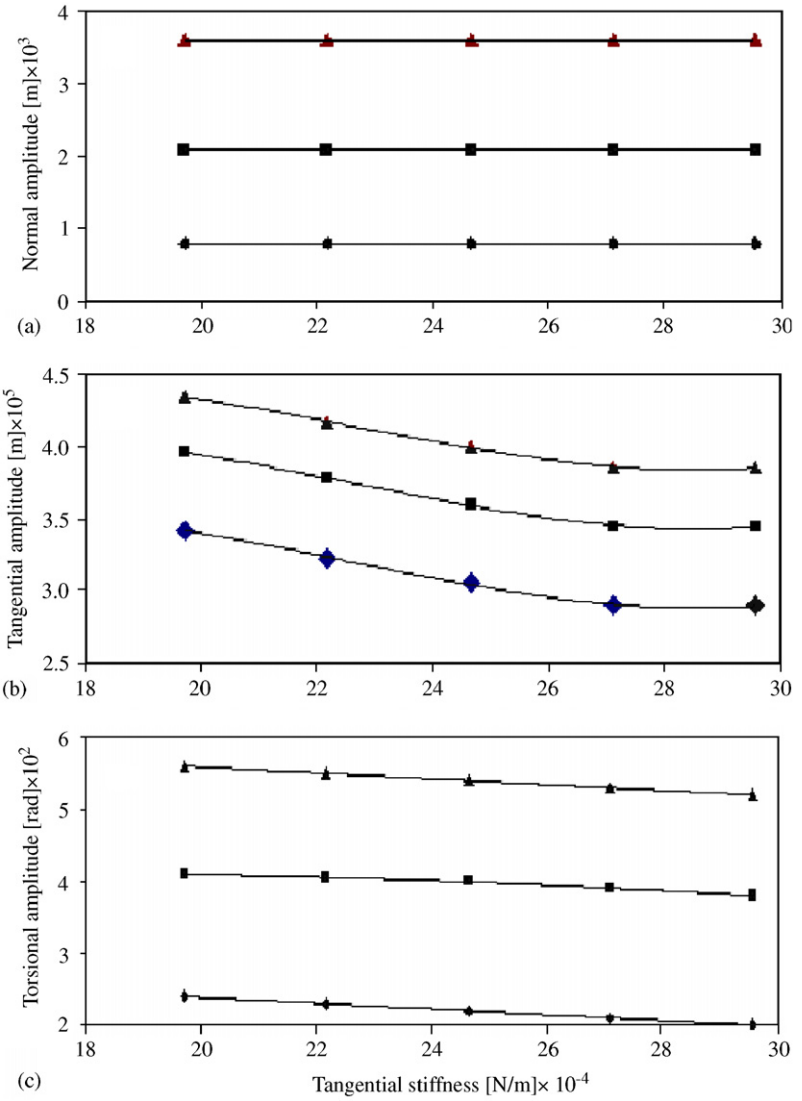

Fig. 9. System steady-state response versus tangential stiffness at 100 rev/min; in the three directions: (a) vertical, (b) horizontal and (c) torsional, at three applied normal forces: (—▲—) 45 N, (—■—) 35 N and (—◆—) 25 N.

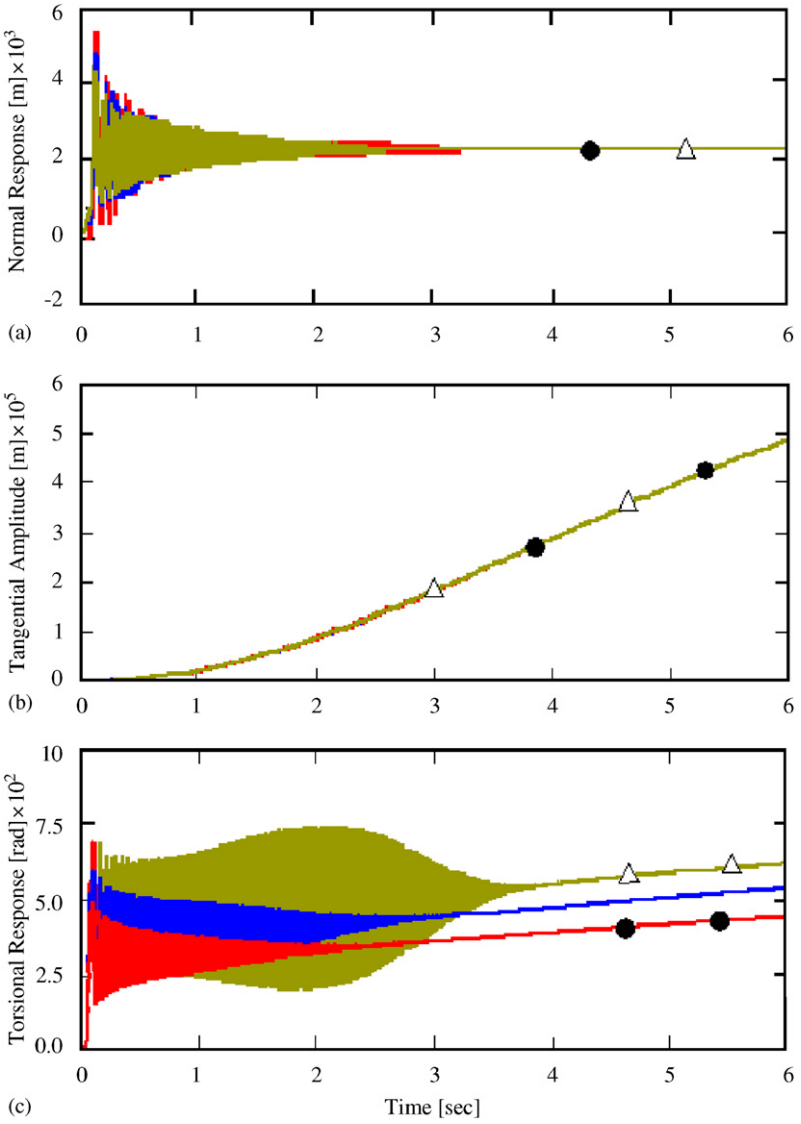

Fig. 10. Effect of varying torsional stiffness k_3 on system response; at 100 rev/min and 35 N applied normal force, in the three directions: (a) vertical, (b) horizontal and (c) torsional. (△——△) −20%, (——) setup value of k_3 and (●——●) +20%.

4.4. *Effect of changing the torsional stiffness on the response*

The effect of changing the torsional stiffness k_3 on the time history of normal, tangential and torsional response amplitudes, at rotational speed of 100 rev/min and normal force of 35 N, is shown in Fig. 10. Figs. 10(a) and (b) show that there is no change in both normal and tangential amplitude of response due to changing the torsional stiffness. On the other hand, Fig. 10(c) shows that the change of the torsional stiffness inversely affects the steady-state torsional amplitude of response.

In Fig. 11, the effect of varying the torsional stiffness k_3 on the steady-state response, at three different normal forces is shown. Figs. 11(a) and (b) show that changing the torsional stiffness has no effect on both normal and tangential amplitude of steady-state response. On the other hand an increase of 10% of the torsional stiffness leads to a decrease of around 8% in the torsional amplitude of steady-state response. Thus, changing the torsional stiffness affects the response in the torsional direction only.

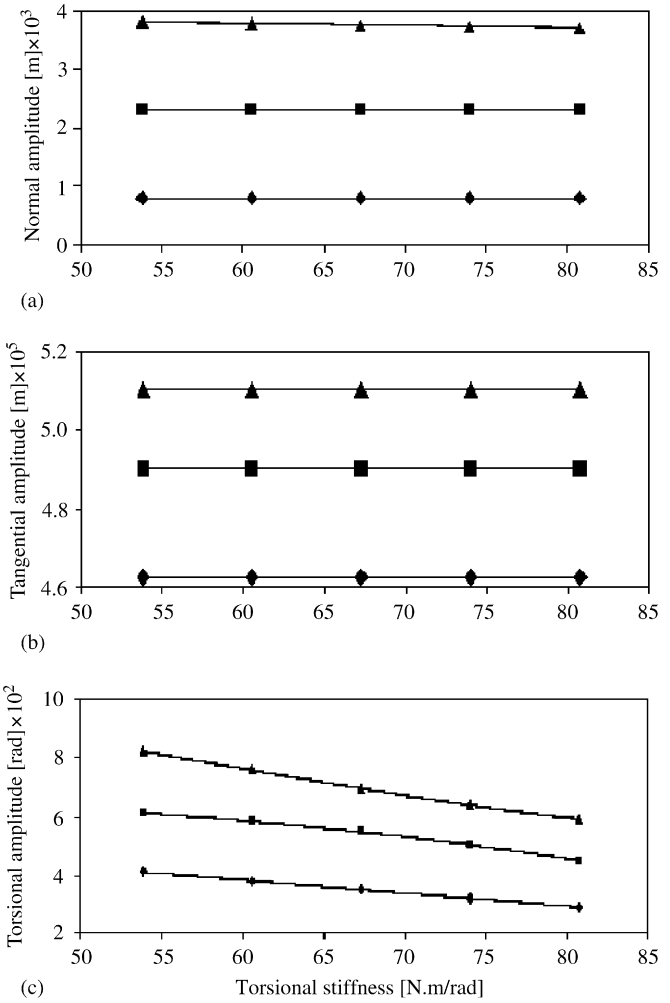

Fig. 11. System response versus torsional stiffness at 100 rev/min; in the three directions: (a) vertical, (b) horizontal and (c) torsional, at three applied normal forces: (—▲—) 45 N, (—■—) 35 N and (—◆—) 25 N.

5. Conclusions

Based on experimental data, a three-degrees-of-freedom model of a pin-on-disk system is presented. The model is used to investigate the effect of varying both the normal force and the system stiffness parameters on the system response in three directions at different speeds.

It is found that at any specific speed, increasing the normal force increases the calculated system response. This is true for the response in all the three directions. Also, increasing the rotational speed of the pin increases the amplitude of system response in the three directions. The validity is proved through the good correlation between the measured sound pressure level and the corresponding calculated system vibrational response in the normal direction.

The change in amplitude of system response is inversely related to changes into stiffness parameters of the system. The change in the normal stiffness influences the amplitude of system response in both normal and torsional directions, while changing the tangential stiffness affects the response in both tangential and torsional directions. On the other hand, varying the torsional stiffness influences the amplitude of system response in the torsional direction only. It is worth to mention that a specific stiffness profoundly affect the

response in its direction. For example, the change in the normal stiffness affects both the normal and the torsional response, with a profound effect on the normal response. So, system geometry and material should be considered during design process regarding its effect on the system dynamic response.

As the effect of changing the different operating parameters on the system response is known, so the thought of controlling such responses is a definite aim for a future work via various means such as passive control.

References

[1] R.P. Jarvis, B. Mills, Vibration-induced by dry friction, *Proceedings of the Institution of Mechanical Engineers* 178 (32) (1963) 847–857.

[2] S.W.E. Earles, C. Lee, Instabilities arising from the frictional interaction of a pin-disk system resulting in noise generation, *Transactions of the American Society of Mechanical Engineers Journal of Engineering for Industry* 98 (1) (1976) 81–86.

[3] S.W.E. Earles, M. Badi, Oscillatory instabilities generated in a double-pin and disk undamped system: a mechanism of disk-brake squeal, *Proceedings of the Institution of Mechanical Engineers C* 198 (1984) 43–49.

[4] S.W.E. Earles, P.W. Chambers, Predicting some effects of damping on the occurrence of disk-brake squeal noise, *ASME Dynamic Systems and Control Division*, Vol. 1, ASME, New York, 1985, pp. 317–323.

[5] S.W.E. Earles, P.W. Chambers, Disk brake squeal noise generation: predicting its dependency on system parameters including damping, *International Journal of Vehicle Design* 8 (1987) 538–552.

[6] J.T. Oden, J.A.C. Martins, Models and computational methods for dynamic friction phenomena, *Computer methods in Applied Mechanics and Engineering* 52 (1985) 527–634.

[7] A.H. Dweib, L.T. D'Souza, Self-exited vibrations induced by dry Friction, Part I: Experimental study, *Journal of Sound and Vibration* 137 (1990) 163–190.

[8] L.T. D'Souza, A.H. Dweib, Self-exited vibrations induced by dry friction, Part II: stability and limit cycles analysis, *Journal of Sound and Vibration* 137 (1990) 163–190.

[9] R.A. Ibrahim, Friction-induced vibration, chatter, squeal, and chaos; Part I: mechanics of friction; Part II: dynamics and modeling, *ASME, Journal of Vibrations and Acoustics* 49 (1992) 107–138.

[10] R.A. Ibrahim, S. Madhavan, S.L. Qiao, W.K. Chang, Experimental investigation of friction-induced noise in disk brake systems, *International Journal of Vehicle Design* 23 (2000) 218–240.

[11] S.L. Qiao, R.A. Ibrahim, Stochastic dynamics of systems with friction-induced vibration, *Journal of Sound and Vibration* 223 (1) (1999) 115–140.

[12] R.A. Ibrahim, Friction-induced noise and related problems in automotive brakes, in: S.G. Pandalai (Ed.), *Recent Research Developments in Sound and Vibration*, Vol. 1, Transworld Research Network, Kerala, India, 2002.

[13] A. Akay, Acoustics of friction, *Journal of Acoustic Society of America* 111 (2002) 1525–1548.

[14] M.N. Emira, H.M. Uras, The influence of external vibrations on friction-induced noise, *Alexandria Engineering Journal* 38 (5) (1999) A341–A355.

[15] N.M. Kinkaid, O.M. O'Reilly, P. Papadopoulos, Automotive disk brake squeal, *Journal of Sound and Vibration* 267 (2003) 105–166.

[16] C.D. Mote Jr., Stability of circular plates subjected to moving loads, *Journal of the Franklin Institute* 290 (1970) 329–344.

[17] W.D. Iwan, T.L. Moeller, The stability of a spinning elastic disk with transverse loading system, *Transaction of the American Society of Mechanical Engineers, Journal of Applied Mechanics* 43 (1976) 485–490.

[18] I.Y. Shen, Response of a stationary damped circular plate under a rotating slider bearing system, *Transaction of the American Society of Mechanical Engineers, Journal of Vibration and Acoustics* 115 (1993) 65–69.

[19] W.W. Tworzydlo, E.B. Becker, J.T. Oden, Numerical modeling of friction-induced vibrations and dynamic stabilities, *ASME, Transaction of Applied Mechanics Reviews* (1994).

[20] K. Shin, M.J. Brennan, J.-E. Oh, C.J. Harris, Analysis of disk brake noise using a two-degree-of-freedom model, *Journal of Sound and Vibration* 254 (5) (2002) 837–848.

[21] J.E. Mottershead, Vibration and friction-induced instability in disks, *Shock Vibration Digest* 30 (1998) 14–31.

[22] H. Ouyang, J.E. Mottershead, Unstable traveling waves in the friction-induced vibration of disks, *Journal of Sound and Vibration* 248 (4) (2001) 768–779.

[23] S.N. Chan, J.E. Mottershead, M.P. Cartmell, Parametric resonances at sub-critical speeds in disks with rotating frictional loads, *Proceedings of the Institution of Mechanical Engineers Part C* 208 (C6) (1994) 417–425.

[24] S.N. Chan, J.E. Mottershead, M.P. Cartmell, Instabilities at sub-critical speeds in disks with rotating frictional follower loads, *Transactions of the American Society of Mechanical Engineers Journal of Vibration and Acoustics* 117 (2) (1995) 240–242.

[25] J.E. Mottershead, S.N. Chan, Flutter instability of circular disks with frictional follower loads, *Journal of Vibration and Acoustic* 117 (1) (1995) 161–163.

[26] H. Ouyang, J.E. Mottershead, M.P. Cartmell, M.I. Friswell, Friction-induced parametric resonances in disks: effect of a negative friction-velocity relationship, *Journal of Sound and Vibration* 209 (1998) 251–264.

[27] H. Ouyang, J.E. Mottershead, D.J. Brookfield, S. James, M.P. Cartmell, A methodology for the determination of dynamic instabilities in a car disk brake, *International Journal of Vehicle Design* 23 (3/4) (2000) 241–262.

[28] H. Ouyang, J.E. Mottershead, D.J. Brookfield, S. James, M.P. Cartmell, T. Kaster, T. Treyde, B. Hirst, R. Allen, Dynamic instabilities in a simple model of a car disk brake, Technical Report 1999-01-3409, SAE, Warrendale, PA, 1999.
[29] H. Ouyang, Q. Cao, J.E. Mottershead, T. Treyde T, Vibration and squeal of a disk brake: modeling and experimental results, *IMechE Journal of Automotive Engineering* 217 (10) (2003) 867–875.
[30] H. Ouyang, J.E. Mottershead, A bounded region of disk-brake vibration instability, *Transactions of the American Society of Mechanical Engineers Journal of Vibration and Acoustics* 123 (4) (2001) 543–545.
[31] W.T. Thomson's, *Theory of Vibration with Applications*, third ed., Prentice-Hall, Inc., Englewood Cliffs, NJ, 1988 pp. 100–102.
[32] R.G. White, J.G. Walker, *Noise and Vibration*, Wiley, New York, 1982 pp. 497–606.